24th Workshop on Crystalline Silicon Solar Cells & Modules: Materials and Processes,
July 27-30, 2014, Breckenridge, USA

Implied V_{oc} determination on IBC cell structure with front floating emitter

Agnes Mewe[#], Kay Cesar, Yu Wu, Nicolas Guillevin, Teun Burgers, Bart Geerligs, Arthur Weeber
ECN Solar Energy, P.O. Box 1, NL-1755 ZG Petten, The Netherlands, [#]mewe@ecn.nl

Abstract
In this paper, we discuss a method to determine the implied V_{oc} as a parameter describing the passivation quality of the diffused and passivated interdigitated structure of our Mercury IBC cell, which features a front floating emitter. We investigated how to accurately determine the implied V_{oc} of the IBC cell structure before metallization from QSSPC lifetime measurements. We found that direct measurement of the implied V_{oc} from carrier density is typically inaccurate in the IBC case. The proposed measurement method is based on determination of the total surface saturation current density (J_o) at high injection level, and using this value to directly calculate the implied V_{oc}. We verified the correspondence of direct and indirect (via J_o) measurements of implied V_{oc} on non-metallized cells with full area front emitter and rear BSF. We find that the verification has a certain level of uncertainty due to the varying level of the bulk J_o, which needs to be resolved before the accuracy of the application to IBC structures can be tested.

IBC device structure: Mercury
Interdigitated back-contact cells are of increasing interest, due to the high efficiency potential, and aesthetics of the resulting modules, and are in development by many parties [1-7]. At ECN we have developed the Mercury cell concept, which is an IBC cell with a front floating emitter (FFE), as shown in Fig. 1a. In our Mercury design, the FFE efficiently transports minority carriers to the collecting rear side emitter and therefore allows wider BSF areas [8]. We manufactured full-size 6 inch IBC Mercury cells with so far 19.5% efficiency [9, to be published], featuring very high J_{sc}. The V_{oc} of the device is currently still slightly below 0.640 V, limiting the cell performance, and is therefore under close examination for routes to improvement. Large recombination contributions in the present cells are ascribed to the considerable metallization fraction and the heavily doped BSF. For analysis and quantification of the recombination losses of the different passivated and contacted areas of the cell, it is very helpful to know the V_{oc} of the complete cell as well as the different contributions of the cell structure before metallization (implied V_{oc}). As an alternative to (implied) V_{oc}, the J_o of half-fabricates and completed cells could be analyzed and compared, but the J_o measurement on a completed cell may not be conveniently possible, so therefore the implied V_{oc} is usually the preferred parameter, which is also more intuitively related to the completed cell quality.

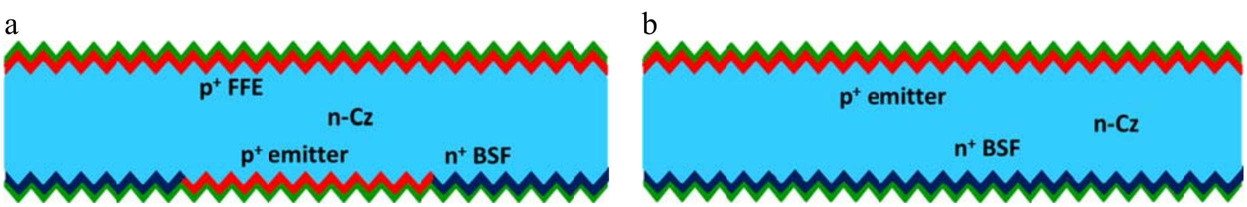

Fig. 1 Schematic cross-sections of a) IBC Mercury, and b) n-Pasha cell structures without metallization.

IBC implied V_{oc} direct measurement in the WCT photoconductance tool

The determination of the implied V_{oc} at 1 sun is normally accomplished by a straightforward photoconductance (Sinton WCT tool) lifetime measurement of a half-fabricate cell structure without metallization. For cell structures with full-area doping of one polarity on a wafer side, such as our n-Pasha cell (Fig. 1b) or for symmetrically doped structures, this direct implied V_{oc} measurement is regularly reported in papers as an indicating parameter for the cell structure quality. However, we observed that the implied V_{oc} of the IBC cell structure is not straightforward to measure in this direct way. For example, resulting values can be higher than the weighted average of the implied V_{oc} of the homogeneous test structures. This is caused by an anomaly in the minority carrier lifetime plot of the IBC samples, including the implied V_{oc} point at 1 sun, as shown in Fig. 2a. This anomaly is not present in the measurement of a front junction n-Pasha cell structure or IBC test structures with large areas of one surface doping type (area is 4x4 cm^2, which is larger than the coil size of 1.8 cm). The non-equilibrium carrier density, minority carrier lifetime, and therefore the implied V_{oc}, at the anomaly are over-estimated. The reason for the over-estimation is that the pn-junctions at the IBC rear side are conducting in light condition, while it is a barrier for conduction in dark condition, as sketched in Fig. 2b. This increase in conductivity is translated to a higher non-equilibrium carrier density in the WCT software, because in the software a conductivity change for varying light level is assumed to be only related to a change in the number of photogenerated carriers. Since the onset of extra conductivity through the pn-junctions as a function of illumination level might be gradual, an approximate correction by using a “light bias” (in reality or simulated in the software) does not work very well.

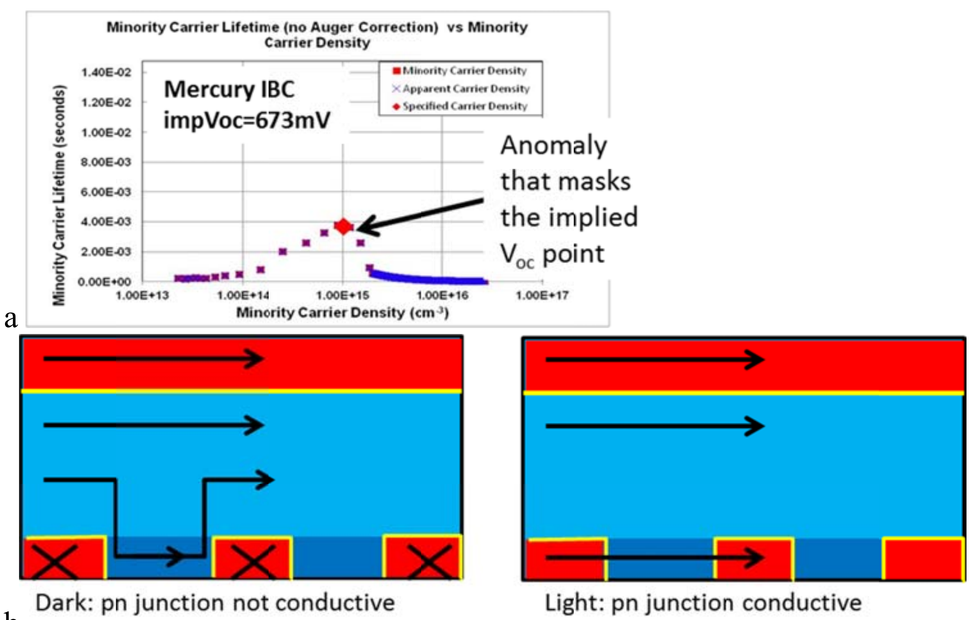

a

b

Fig. 2 Implied V_{oc} determination of IBC structure with a) the anomaly at the V_{oc} evaluation point leading to overestimation of the implied V_{oc}, b) the mechanism of the pn conductivity switch in light, causing an extra increase in conductivity in the conductivity curve that is measured during the Sinton QSSPC light flash.

Solution to conductivity-switch related anomaly in lifetime curve: use J_o

At high injection, the effect of pn-junction switching disappears as the conductivity contribution of carrier concentration Δn in the wafer becomes dominant and the conductivity of the pn-junction is constant. The J_o of the sample surface can therefore be correctly evaluated at high injection, at typically 10 times the doping level of the bulk wafer material.

$$impV_{oc} = \frac{nKT}{q}\ln(\frac{J_L}{J_0}+1)$$

Fig. 3 Calculation of implied V_{oc} from the measured J_o.

We developed a measurement protocol to determine the J_o correctly for each sample surface, which involves J_o determination at high injection. The J_o value from the QSSPC measurement plus a suitably chosen value for the bulk saturation current, is inserted into the V_{oc} equation as shown in Fig. 3. Choosing an appropriate value is not trivial, but we assumed that the $J_{o,bulk}$ value in case of a gettered wafer would be 35 fAcm^{-2}, and in case of a non-gettered wafer 150 fAcm^{-2}. For J_L the typical short circuit current density of n-type n-Pasha or IBC cells is taken (40 mAcm^{-2}). This method is tested on a symmetrical $p^+/n/p^+$ structure (emitter-emitter) and on a $p^+/n/n^+$ (emitter-BSF) cell structure on the same wafer material, comparing both the (standard) direct implied V_{oc} method as well as the method of J_o determination and subsequent calculation of the implied V_{oc}. This procedure is schematically sketched in Fig. 4.

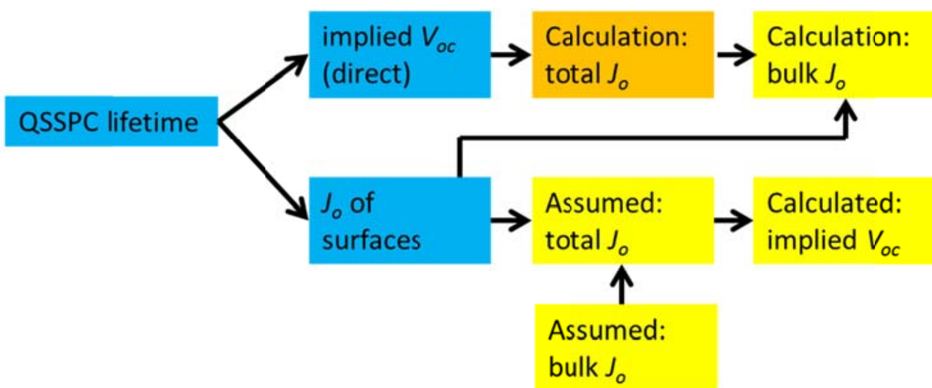

Fig. 4 Schematic sketch of the measured and derived parameters of J_o and implied V_{oc}, as listed in Table 1.

The results are summarized in Table 1. It becomes directly clear that there is a mismatch between the assumed $J_{o,bulk}$ and the calculated $J_{o,bulk}$ which was derived from the total J_o (through implied V_{oc}) and the surface J_o. Deriving the J_o of the bulk in such a way is still under discussion.

Table 1 Results of direct measurement and calculation from J_o of the implied V_{oc} for full-size uniform diffusions and from IBC Mercury structures with different rear design. In between brackets the weighted average of the J_o values from the test structures.

structure	**direct *i*-V_{oc} [V]**	**J_o total calculated [fAcm^{-2}]**	**J_o surfaces 2 sides [fAcm^{-2}]**	**J_o bulk calculated [fAcm^{-2}]**	**J_o bulk assumed [fAcm^{-2}]**	***i*-V_{oc} calculated [V]**
$p^+/n/p^+$	0.650	423	143	281	150	0.660
$p^+/n/n^+$	0.673	174	105	68	35	0.679
Mercury 1	NA		224 (252)		?	
Mercury 2	NA		254 (287)		?	

We verified this method on the $p^+/n/p^+$ structures (emitter-emitter) and the $p^+/n/n^+$ (emitter-BSF) test structures that were fabricated in the same process as our Mercury cells. Also in this case we observed a mismatch between the directly measured implied V_{oc} and the implied V_{oc} that is calculated as a sum of the measured J_o of the surfaces plus an assumed $J_{o,bulk}$ value, which is especially large for the emitter-BSF structure. The surface J_o of two Mercury IBC structures with different rear design was determined, and these values give an estimate of the quality of the diffused surfaces. We observed that the measured surface J_o is slightly lower than the weighted average of the test structures (values in brackets). This is not yet understood. To determine the implied V_{oc} of the IBC structures, we need to know the bulk J_o of the wafer material. As shown in Table 1 and indicated by the test structures, this value seems to vary, and may depend on the processing history of the material. The question now is how to translate the $J_{o,bulk}$ values of uniform diffusions, derived from the implied V_{oc}, into $J_{o,bulk}$ values of the IBC structures. Due to the small feature sizes of the interdigitated structure, it might not be possible to use the weighted average.

Conclusion

We discussed a method to determine implied V_{oc} as a parameter describing the passivation quality of the Mercury IBC cell, by measuring the J_o values and calculating the implied V_{oc}. Verification of the method by measurements on different cell structures reveals differences in bulk J_o for the different structures that are present in the IBC cell. It will be further investigated how to solve this uncertainty in the determination of the bulk J_o of the IBC cell.

Acknowledgements

We thank Ron Sinton for helpful discussions and advice. This work was supported by the IBCool project; we thank the Dutch Ministry of E&I for funding.

References

[1] Smith et al. “SunPower’s Maxeon Gen III solar cell: High Efficiency and Energy Yield”, Proc. 39th IEEE PVSC, Tampa, 2013

[2] Fong et al. , “Optimisation of n+ diffusion and contact size of IBC solar cells”, 28th EU-PVSEC, Paris (2013)

[3] B. O’Sullivan et al, “Process simplification for high efficiency, small area interdigitated back contact silicon solar cells”, 28th EU-PVSEC, Paris (2013)

[4] Bosch SE, press release (2013).

[5] C.B. Mo et al., Proc. 27nd EU-PVSEC, Frankfurt, Germany (2012).

[6] A. Halm et al.“The Zebra Cell Concept - Large Area n-Type Interdigitated Back Contact Solar Cells and One-Cell Modules Fabricated Using Standard Industrial Processing Equipment”, 27nd EU-PVSEC, Frankfurt, Germany (2012).

[7] Dong et al., “High-Efficiency Full Back Contacted Cells Using Industrial Processes” Proc. 39th IEEE PVSC, Tampa, 2013

[8] Cesar et al., Mercury: A Back Junction Back Contact Front Floating Emitter Cell With Novel Design For High Efficiency And Simplified Processing, 2014, SiliconPV, ‘s Hertogenbosch

[9] Cesar et al., 2014, EUPVSEC (to be published)